

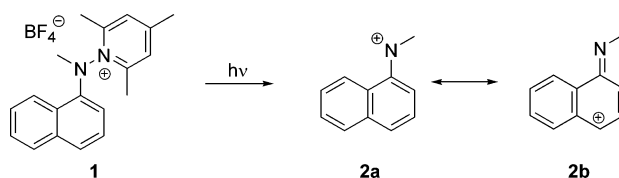
## Photogenerated *N*-Methyl-*N*-1-naphthylnitrenium Ion: Laser Flash Photolysis, Trapping Rates, and Product Study

Andrew C. Kung and Daniel E. Falvey\*

Department of Chemistry and Biochemistry, University of Maryland, College Park, Maryland 20742-2021

*falvey@umd.edu*

Received December 20, 2004



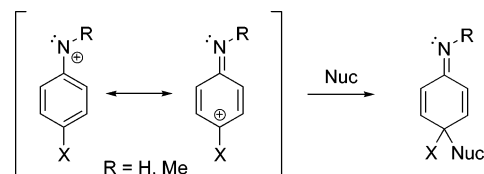
*N*-Methyl-*N*-1-naphthylnitrenium ion (**2**) was generated through photolysis of 1-(*N*-methyl-*N*-(1-naphthyl)amino)-2,4,6-trimethylpyridinium tetrafluoroborate (**1**). Laser flash photolysis (LFP) with time-resolved UV-vis (TRUV) detection as well as photoproduct analysis verified that the expected nitrenium ion was formed cleanly and rapidly following photolysis. Consistent with an earlier study, which used competitive trapping methods (Novak, M. et al. *J. Org. Chem.* **1999**, *64*, 6023–6031), it is found that **2** reacts rapidly with a variety of nucleophiles. The high reactivity of **2** relative to other arylnitrenium ions is discussed in terms of steric and electronic effects.

### Introduction

Nitrenium ions are divalent, electron-deficient nitrogen species ( $\text{NR}_1\text{R}_2^+$ ), isoelectronic to carbocations, carbenes, and nitrenes.<sup>1</sup> Nitrenium ions are interesting due to (1) their utility in synthesis,<sup>2,3</sup> (2) their suspected intermediacy in the synthesis of conducting (poly)aniline,<sup>4,5</sup> and (3) their role in DNA damage caused by enzymatically activated arylamine carcinogens.<sup>6–8</sup>

Arylnitrenium ions generally have short lifetimes in solution. Monoarylnitrenium ions with  $\pi$ -donating (Scheme 1: X = phenyl or alkoxy) substituents in the para position are highly stabilized to addition of simple nucleophiles, such as water. The latter adds to the ring carbons as illustrated in Scheme 1.

### SCHEME 1. General Addition of Nucleophiles to Nitrenium Ions



In contrast,  $\pi$ -nucleophiles, such as guanine bases in DNA, can add to the nitrogen. Monoarylnitrenium ions without the para-substitution pattern have subnanosecond lifetimes in solution. The stability of arylnitrenium ions with respect to nucleophiles has important implications in chemical toxicology. As a rule, it seems that arylnitrenium ions lacking stabilizing substituents in the para position react so rapidly with water that their ability to damage DNA is negligible. In contrast, conjugated aryl substituents in the para position stabilize arylnitrenium ions to water addition and leave its reactivity to aromatic nucleophiles (such as DNA bases) relatively unaffected. This leads to the question whether this observation is a steric or an electronic effect.

It is reasonable to suspect that increasing the  $\pi$ -conjugation of the system would stabilize the nitrenium ion, prolonging its lifetime. To test this hypothesis, we turned our attention to *N*-methyl-*N*-1-naphthylnitrenium ion (**2**). This nitrenium ion benefits from the stabilizing electronic effect of benzannulation, while keeping the para position open. This is in contrast to **10**, which has a  $\pi$ -conjugating

\* To whom correspondence should be addressed. Fax: (301) 314-9121.

(1) Falvey, D. E. In *Reactive Intermediate Chemistry*; Moss, R. A., Platz, M. S., Jones, M., Jr., Eds.; John Wiley & Sons: Hoboken, NJ, 2004; pp 593–650.

(2) Kikugawa, Y.; Kawase, M. *J. Am. Chem. Soc.* **1984**, *106*, 5728–5729.

(3) Wardrop, D. J.; Zhang, W. M. *Org. Lett.* **2001**, *3*, 2353–2356.

(4) Ding, Y.; Padias, A. B.; Hall, J. H. K. *J. Polym. Sci. Polym. Chem.* **1999**, *37*, 2569–2579.

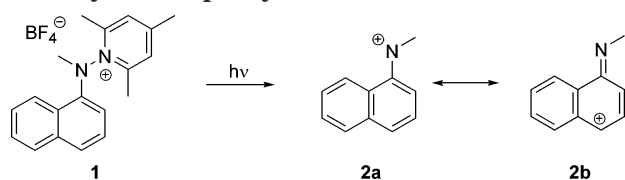
(5) Wei, Y.; Tang, X.; Sun, Y. *J. Polym. Sci. Polym. Chem.* **1989**, *27*, 2385–2396.

(6) Miller, J. A. *Cancer Res.* **1970**, *30*, 559–576.

(7) Kadlubar, F. F. In *DNA Adducts: Identification and Biological Significance*; Hemmink, K. K. A., Shugar, D. E. G., Kadlubar, F. F., Segerback, D., Bartsch, H., Eds.; University Press: Oxford, UK, 1994; pp 199–216.

(8) Schut, H. A. J.; Snyderwine, E. G. *Carcinogenesis* **1999**, *20*, 353–368.

**SCHEME 2. Photolysis of 1-(*N*-Methyl-*N*-(1-naphthyl)Amino)-2,4,6-trimethylpyridinium Tetrafluoroborate (1) Yielding *N*-Methyl-*N*-1-naphthylnitrenium Ion (2)**



phenyl group at the para position, which also increases sterics. Thus, we can study the electronic effect of  $\pi$ -conjugation in the absence of significant steric effects and determine which factor takes precedence in this *N*-methyl-*N*-1-naphthylnitrenium ion system (2).

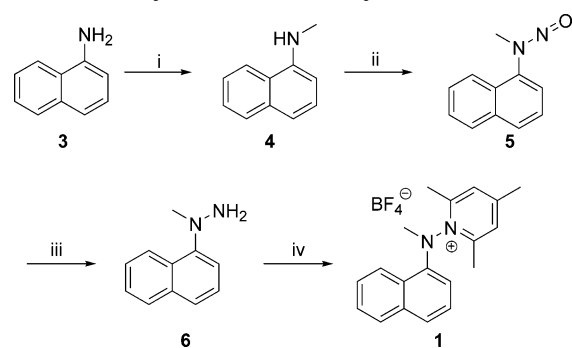
## Results

**1. Synthesis of Photochemical Precursor to the Nitrenium Ion.** There are two widely used photochemical routes for generating nitrenium ions. One method is to photolyze an azide in aqueous solution. Under these conditions, the resulting singlet nitrene can be rapidly protonated, yielding the corresponding nitrenium ion.<sup>9,10</sup> Thus, we examined the photolysis of 1-naphthyl azide in aqueous solution by laser flash photolysis (LFP). When these experiments were carried out, the observed signals did not differ significantly from those generated in aprotic solution. In fact, the signals we detected have been previously observed and are attributed to the well-known ring expansion intermediates from the nitrene.<sup>11–13</sup> For this reason we conclude that the unimolecular reactions of the singlet nitrene, including cyclization and intersystem crossing, are faster than the competing proton transfer. Therefore, we used another precursor to generate the nitrenium ion.

Previous studies have shown that arylnitrenium ions can be cleanly generated through photolysis from the corresponding substituted *N*-amino pyridinium salts<sup>14–17</sup> (Scheme 2). Thus, *N*-methyl-1-aminonaphthalene (4) was synthesized by direct methylation of 3 with iodomethane and then nitrosated to give *N*-methyl-*N*-nitroso-1-aminonaphthalene (5) (Scheme 3). The latter was reduced to generate 1-methyl-1-(1-naphthyl)hydrazine (6). A substoichiometric amount of freshly prepared 2,4,6-trimethylpyrylium tetrafluoroborate was added in situ to the reduction mixture, yielding the final pyridinium salt (1). The pyridinium salt was then recrystallized, first from EtOH, then from MeOH.

**2. Stable Photoproducts.** Photolysis of 1 gives products characteristic of those expected from a singlet

**SCHEME 3. Synthesis of the Pyridinium Salt 1<sup>a</sup>**



<sup>a</sup> Reagents: (i) MeI, MeCN; (ii) NaNO<sub>2</sub>, HCl, H<sub>2</sub>O on ice bath; (iii) Zn, EtOH, AcOH, H<sub>2</sub>O on ice bath; (iv) 2,4,6-trimethylpyrylium tetrafluoroborate, EtOH.

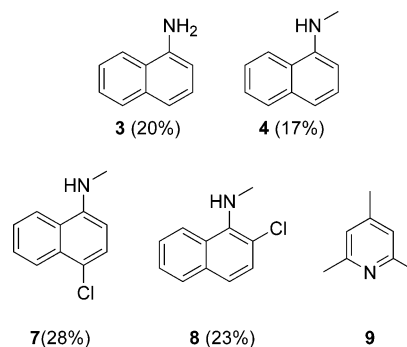


**FIGURE 1.** Photoproducts from 1 and 5.42 mM Cl<sup>-</sup> in MeCN. Percentages are based on gravimetric analysis.

arylnitrenium ion. As a general rule, all but the most stable nitrenium ions react with anionic nucleophiles, such as chloride, at the diffusion-limited rate.<sup>18,19</sup> Pyridinium salt (1) was photolyzed with 5.42 mM *n*Bu<sub>4</sub>NCl, in MeCN at 355 nm. From the photolysis mixture five products were detected (Figure 1): 1-aminonaphthalene (3), *N*-methyl-1-aminonaphthalene (4), 4-chloro-*N*-methyl-*N*-1-aminonaphthalene (7), 2-chloro-*N*-methyl-*N*-1-aminonaphthalene (8), and 2,4,6-collidine (9). Compounds 3, 4, and 7 were isolated and characterized by <sup>1</sup>H NMR. Photoproduct 8 was isolated and characterized through <sup>1</sup>H NMR, <sup>13</sup>C NMR, COSY-<sup>1</sup>H NMR, and HRMS. 2,4,6-Collidine (9) was characterized through GC/MS.

All of the products are consistent with the formation of an arylnitrenium ion. Photoproducts 7 and 8 are formed through the nucleophilic addition of chloride at the ortho and para positions to the nitrogen and are analogous to adducts of similar arylnitrenium ions such as *N*-methyl-*N*-phenylnitrenium ion.<sup>20</sup>

Product 3 apparently forms through a 1,2-hydride shift from the *N*-methyl group to the electron deficient nitrogen. A similar process has been observed with *N*-methyl-*N*-phenylnitrenium ion.<sup>20</sup> The hydride shift would form the iminium ion, which hydrolyzes upon aqueous workup to yield 3.

(18) Kung, A. C.; Chiapperino, D.; Falvey, D. E. *Photochem. Photobiol. Sci.* **2003**, *2*, 1205–1208.

(19) McIlroy, S.; Moran, R. J.; Falvey, D. E. *J. Phys. Chem. A* **2000**, *104*, 11154–11158.

(20) Chiapperino, D.; Falvey, D. E. *J. Phys. Org. Chem.* **1997**, *10*, 917–924.

(9) McClelland, R. A.; Kahley, M. J.; Davidse, P. A.; Hadzialic, G. *J. Am. Chem. Soc.* **1996**, *118*, 4794–4803.

(10) Ren, D.; McClelland, R. A. *Can. J. Chem.* **1998**, *76*, 78–84.

(11) Schrock, A. K.; Schuster, G. B. *J. Am. Chem. Soc.* **1984**, *106*, 5234–5240.

(12) Tsao, M. L.; Platz, M. S. *J. Phys. Chem. A* **2004**, *108*, 1169–1176.

(13) Maltsev, A.; Bally, T.; Tsao, M. L.; Platz, M. S.; Kuhn, A.; Vosswinkel, M.; Wentrup, C. *J. Am. Chem. Soc.* **2004**, *126*, 237–249.

(14) Abramovitch, R. A.; Evertz, K.; Huttner, G.; Gibson, H. H.; Weems, H. G. *J. Chem. Soc., Chem. Commun.* **1988**, 325–327.

(15) Takeuchi, H. *J. Chem. Soc., Chem. Commun.* **1987**, 961–963.

(16) Moran, R. J.; Falvey, D. E. *J. Am. Chem. Soc.* **1996**, *118*, 8965–8966.

(17) Zhu, P.; Ong, S. Y.; Chan, P. Y.; Poon, Y. F.; Leung, K. H.; Phillips, D. L. *Chem. Eur. J.* **2001**, *7*, 4928–4936.

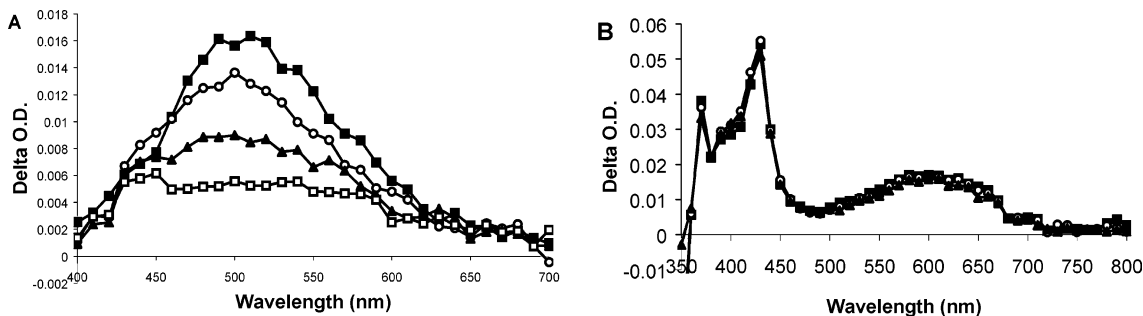


**FIGURE 2.** Transient UV-vis absorption spectra generated from LFP (355 nm, 4–6 ns, 8–10 mJ/pulse) taken 0.2 (■), 0.4 (○), 0.8 (▲), and 1.6 (□)  $\mu$ s after the laser pulse of (A) **1** in MeCN and (B) **3** in the presence of 1,4-DCB in MeCN. This spectrum is assigned to  $\mathbf{3}^{+\cdot}$  (see text).

Product **4** could occur through hydrogen abstraction from the solvent or through secondary photolysis/electron-transfer pathway of either of the chloro adducts.<sup>20</sup> The 4-chloro or 2-chloro adduct may be irradiated to homolytically cleave the C–Cl bond. This would be followed by an H-atom abstraction to yield the monomethylated product **4**.

Substitution at the 2- and 4-positions is supported by the observations made by the Novak and Underwood groups through solvolysis reactions of differently *N*-substituted 1-aminonaphthalenes.<sup>21,22</sup>

**3. Laser Flash Photolysis: Time-Resolved UV-Vis (LFP-TRUV).** LFP (355 nm, 4–6 ns, 8–10 mJ/pulse) of **1**, in MeCN, gives a short-lived visible absorption band with  $\lambda_{\text{max}} = 500$  nm and has a lifetime of 835 ns, as shown in Figure 2A. This transient signal is ascribed to the singlet arylnitrenium ion since the observed transient signal is insensitive to the presence of  $\text{O}_2$  and reacts rapidly with nucleophiles (see below).

Also considered was the possibility that the observed signal was due to the radical cation of **3**. To test for this possibility, radical cation  $\mathbf{3}^{+\cdot}$  was generated through LFP of amine **3** in the presence of 1,4-dicyanobenzene (1,4-DCB). Excited-state electron transfer from the amine to 1,4-DCB can occur to generate  $\mathbf{3}^{+\cdot}$  and 1,4-DCB $^{\cdot-}$ . The resulting LFP spectrum is shown in Figure 2B and shows an absorption band at 624 nm, which is much different from Figure 2A. This difference in absorption shows that the absorption at 500 nm of Figure 2A is not due to the radical cation species of the precursor. The signals at 395 and 427 nm are due to the radical anion of 1,4-DCB.<sup>23</sup>

**4. Trapping Rates.** LFP was used to characterize the rate constants for reaction of *N*-methyl-*N*-(1-naphthyl)-nitrenium ion (**2**) with different classes of nucleophiles ( $k_{\text{nuc}}$ ) (Table 1). The trapping rate constants were determined from the observation of the nitrenium ion's absorption band at 500 nm with varying concentrations of nucleophile. In each case, the pseudo-first-order decay rates were found to depend in a linear fashion on the concentration of nucleophile. Previous studies have shown that anionic nucleophiles, such as chloride and azide, have trapping rate constants near the diffusion limit.<sup>9,18</sup>

**TABLE 1.** Observed Second-Order Trapping Rate Constants ( $k_{\text{nuc}}$ ) of Different Classes of Nucleophiles with Nitrenium Ions **2** and **10**<sup>18,24</sup>

nucleophile	$k_{\text{nuc}}$ ( $\text{M}^{-1} \text{s}^{-1}$ )	
	<b>2</b>	<b>10</b>
chloride ion <sup>a</sup>	$(2.7 \pm 0.02) \times 10^{10}$	$(7.7 \pm 1.2) \times 10^9$
$\text{Et}_3\text{N}$	$(1.1 \pm 0.05) \times 10^{10}$	$(3.0 \pm 0.4) \times 10^9$
<i>n</i> BuNH <sub>2</sub>	$(1.0 \pm 0.2) \times 10^{10}$	$(5.8 \pm 0.2) \times 10^9$
<i>t</i> BuNH <sub>2</sub>	$(1.0 \pm 0.07) \times 10^{10}$	$(3.8 \pm 0.6) \times 10^9$
aniline	$(9.6 \pm 1.6) \times 10^9$	$(1.18 \pm 0.2) \times 10^{10}$
DABCO	$(8.7 \pm 0.9) \times 10^9$	$(8.8 \pm 0.3) \times 10^9$
diisopropylamine	$(8.8 \pm 0.6) \times 10^9$	$(1.59 \pm 0.02) \times 10^9$
MeOH	$(1.6 \pm 0.3) \times 10^9$	$(3.8 \pm 1.1) \times 10^5$
EtOH	$(7.8 \pm 1.0) \times 10^8$	$(3.0 \pm 0.1) \times 10^5$
H <sub>2</sub> O	$(1.7 \pm 1.4) \times 10^8$	$(9.3 \pm 0.6) \times 10^4$

<sup>a</sup> The source of  $\text{Cl}^-$  was  $\text{Bu}_4\text{NCl}$ .

Amines tend to have trapping rate constants that are faster than those of alcohols, which are faster than that of water. In the present case, the strongest nucleophile, chloride, has a trapping rate constant near the diffusion limit of MeCN ( $2 \times 10^{10} \text{ M}^{-1} \text{ s}^{-1}$ ). This general trend is seen with the trapping rate constants for arylnitrenium ions **2** and *N*-(4-biphenyl)-*N*-methylnitrenium ion (**10**), listed in Table 1. The precursor to **10** was previously synthesized and studied in these labs.<sup>24,25</sup> The less sterically hindered amines, (*n*BuNH<sub>2</sub>, *t*BuNH<sub>2</sub>, and Et<sub>3</sub>N) have rate constants around  $1.0 \times 10^{10} \text{ M}^{-1} \text{ s}^{-1}$ .

In contrast, the more hindered amines (DABCO, *i*Pr<sub>2</sub>NH, and aniline) have trapping rate constants that are slightly slower than those of the less hindered amines. The amine trapping rate constants are faster than those of the alcohols tested (MeOH, EtOH, and H<sub>2</sub>O). It can be seen that water has the slowest trapping rate constant while EtOH is slightly faster than water. MeOH, the less hindered alcohol, has the fastest trapping rate constants of the alcohols at  $1.6(\pm 0.3) \times 10^9 \text{ M}^{-1} \text{ s}^{-1}$ .

It is interesting to contrast the reactivity of **2** to that of the 4-biphenyl analogue, **10**. The latter species is representative of the 4-arylphenylnitrenium ions, a class that is well-known to be involved in carcinogenic DNA damage. Table 1 compares the rate data from this study with those for **10** derived from an earlier study. It is clear from this listing that **10** is less reactive and more

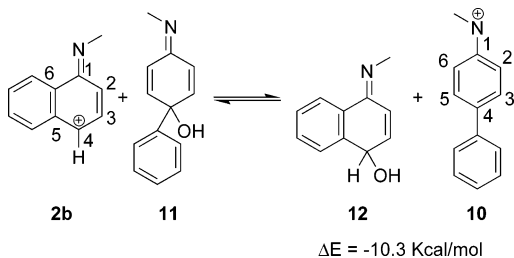
(21) Novak, M.; VandeWater, A. J.; Brown, A. J.; Sanzenbacher, S. A.; Hunt, L. A.; Kolb, B. A.; Brooks, M. E. *J. Org. Chem.* **1999**, *64*, 6023–6031.

(22) Underwood, G. R.; Davidson, C. M. *J. Chem. Soc., Chem. Commun.* **1985**, 555–556.

(23) Shida, T. *Electronic Absorption Spectra of Radical Ions*; Elsevier Science Publishers: New York, 1988.

(24) Chiapperino, D.; McIlroy, S.; Falvey, D. E. *J. Am. Chem. Soc.* **2002**, *124*, 3567–3577.

(25) Srivastava, S.; Ruane, P. H.; Toscano, J. P.; Sullivan, M. B.; Cramer, C. J.; Chiapperino, D.; Reed, E. C.; Falvey, D. E. *J. Am. Chem. Soc.* **2000**, *122*, 8271–8278.

**SCHEME 4. Isodesmic Reaction of 2 and 10 with Water**


selective toward nucleophiles than **2**. For example, **2** reacts ca.  $10^3$  more rapidly with  $\text{H}_2\text{O}$  than does **10**. To examine these differences further density functional theory (DFT) calculations (B3LYP/6-31G(d,p)) were carried out on the two nitrenium ions as well as their hydroxide adducts **11** and **12** (Scheme 4).

A simple analysis of charge distributions and geometries in these two ions leads to the counterfactual expectation that **10** would be more reactive than **2**. In **10**, the positive charge is more strongly localized at the reactive center. Analysis of the charge distribution in both species by using the generalized atomic polar tensor (GAPT) methods reveals a larger charge (+1.104) on the para carbon of the less reactive aryl nitrenium ion **10** than on the corresponding carbon of the more reactive aryl nitrenium ion (+0.670) (Figure 3). Likewise, with respect

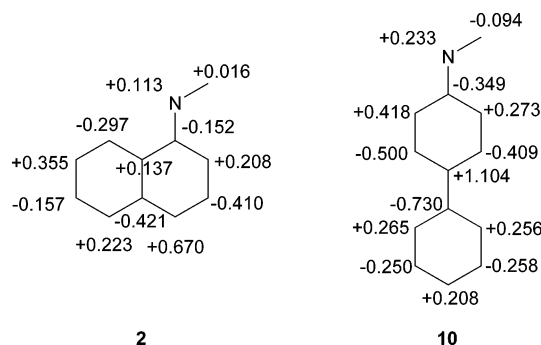


**FIGURE 3.** Generalized atomic polarization tensors (GAPT) charge distribution of **2** and **10**.

to geometries, **10** shows a higher degree of bond length alternation, and thus cyclohexadienyl cation character, than does **2**. In an ideal benzene structure, such as **2a**, all of the ring C–C bonds would be nearly equal, whereas in a 1,4-cyclohexadienyl cation, such as **2b**, the 1–2, 3–4, 4–5, and 6–1 bond lengths would be longer than 2–3 and 5–6. This is the case for both species. For **2** the difference between the average of the four long bonds and the average of the two short bonds is only 0.035 Å, whereas for **10** this value is 0.088 Å.

One obvious difference between **2** and **10** is the degree of steric hindrance to substitution. This makes it tempting to attribute the reactivity differences to entirely steric effects. However, additional examples show that this cannot be a complete explanation. For example, McClelland and Ren used LFP methods to measure aqueous lifetimes for a series of 4'-substituted biphenyl nitrenium ions.<sup>10</sup> In these examples the 4'-substituent can be presumed to have a negligible steric effect on the addition reaction. A linear free energy analysis of these rate

constants using the Hammett substituent parameter  $\sigma^+$  gives a  $\rho$  value of +1.8, indicating that there is a measurable electronic effect on the reactivity within this series. Likewise 4-methyl and 4-halo analogues of **10** are much more reactive than the latter,<sup>18</sup> even though these substituents exert comparable steric barriers to addition.

It seems that a complete explanation for the differences between **2** and **10** requires consideration of both the nitrenium ions and the adducts. One stabilizing effect in **10** is the conjugation of the phenyl substituent to the aryl nitrenium ion ring. This conjugation is lost when addition occurs at the 4-position. We note that the C–C bond joining the phenyl ring to the aryl nitrenium ion center lengthens by nearly 0.1 Å upon addition of water. Likewise, the phenyl ring twists from a nearly coplanar dihedral of 20° in the nitrenium ion to being nearly perpendicular in the adduct. This change in the dihedral angle has been observed via calculations of analogous systems.<sup>26,27</sup> In contrast, **2** does not reorganize to nearly that extent upon addition of water. In the latter system the major change seems to be the restoration of aromaticity to the fused benzene ring.

Novak and Lin analyzed a series of experimental azide/water selectivity ratios (*S*) for a large number of aryl nitrenium ions.<sup>26</sup> This ratio is derived from product analysis data where the nitrenium ions in question were generated in aqueous solution. If one assumes that azide trapping is diffusion limited for the series of nitrenium ions being examined, then *S* is a reasonable proxy for the rate constant for addition of water to these intermediates. These values correlated reasonably well with theoretical (HF/3-21G//6-31G\*) relative hydroxide addition energies, derived from a series of isodesmic hydroxide transfer reactions. We carried out DFT B3LYP/6-31G(d,p) calculations on both **2** and **10**, as well as the initial adducts derived from addition of water to the para positions (**11** and **12**, respectively) (Scheme 4). The energies from these computations agree reasonably well with those given by Novak and Lin. For example, the B3LYP  $\Delta E$  value for the isodesmic reaction involving **2** and **10** is  $-10.3 \text{ kcal/mol}$ , which compares favorably to the HF value of  $-10.8 \text{ kcal/mol}$  (in the latter case, the nonaryl substituents are acetyl rather than methyl). Thus, both DFT and HF agree that the 1-naphthyl derivatives are far less stable with respect to addition of water than are the 4-biphenyl derivatives. We were unable to directly determine the lifetime of **2** in aqueous solution; however, the high  $k_{\text{nuc}}$  value derived in MeCN solution implies that **2** would have a subnanosecond lifetime in aqueous solution.

**Conclusions.** The *N*-methyl-*N*-(1-naphthyl)nitrenium ion (**2**) can be generated through photolysis of the corresponding *N*-pyridinium ion and characterized by using laser flash photolysis. Kinetic trapping data indicate that this species is much more reactive to simple nucleophiles, including water, than similar 4-substituted phenyl nitrenium ions. Thus, it is reasonable to infer that *N*-methyl-*N*-(1-naphthyl)nitrenium ions would have a very short lifetime in an aqueous environment and be only weakly mutagenic, if at all.<sup>28,29</sup> This would be consistent with earlier animal studies.<sup>30,31</sup>

(26) Novak, M.; Lin, J. J. *Org. Chem.* **1999**, *64*, 6032–6040.

(27) Ford, G. P.; Herman, P. S. *Chem. Biol. Interact.* **1992**, *81*, 1–18.

## Experimental Methods

**Calculations.** All geometry optimizations and vibrational frequency calculations were carried out with the Gaussian 03 suite of programs.<sup>32</sup> The values in Figure 3 and Scheme 4 were calculated by using density functional theory, and in particular the hybrid B3LYP functional, comprised of Becke's B3 three-parameter gradient-corrected exchange functional<sup>33,34</sup> with the LYP correlation functional of Lee, Yang, and Parr<sup>35</sup> as originally described by Stephens et al.<sup>36</sup> For these calculations, the 6-31G(d,p) basis set<sup>37</sup> was employed. The GAPT method for allocating partial charges has been described elsewhere.<sup>38</sup>

**LFP-TRUV.** Data from the laser flash photolysis with time-resolved ultraviolet–visible absorption detection experiments were collected with use of a Nd:YAG laser as the pulsed excitation source. Second, third, and fourth harmonic generator crystals were used to create output wavelengths at 355 and 266 nm. The transient absorptions were monitored with use of a probe beam from a 350-W Xe arc lamp passed through the sample cuvette perpendicular to the excitation beam. Transient waveforms were recorded with a digital oscilloscope, which digitizes at a rate of 1 point/10 ns with a bandwidth of 350 MHz. Samples for pulsed irradiation were prepared such that the OD (optical density) of the photolabile substrate was approximately 2.0 at the excitation wavelength employed.

**LFP-TRUV: Radical Cation.** A stock solution of substrate was made with MeCN, such that the OD at the excitation wavelength was between 1.5 and 2.5. This would ensure that the substrate would absorb the pump pulsed beam and undergo photolysis. The concentration of the one-electron acceptor (1,4-DCB) was calculated by using the Stern–Volmer equation. The spectral analysis was performed as described above in LFP-TRUV.

**Trapping Rate Constants.** A stock solution of substrate was made with MeCN, such that the OD at the excitation wavelength was between 1.5 and 2.5. This would ensure that the substrate would absorb the pump pulsed beam and undergo photolysis. A 3-mL sample was transferred by syringe to a quartz cuvette and photolyzed without trap to get the decay rate without any trap. Trap from a millimolar stock solution in MeCN was added to the sample via a microliter syringe in small volumes, usually 10 to 20  $\mu$ L, and photolyzed

to observe the new rate of decay. Consecutive additions of trap were monitored to collect many data points. These data points were then subjected to linear regression to calculate the trapping rate. The resulting trapping rate was reported with errors that were determined with a 95% confidence interval with Microsoft Excel 98 computer software.

**Photoproduct Analysis.** A solution of 245 mg (0.675 mmol) of **1** in 300 mL of MeCN was prepared and stirred for 10 min. To this solution, 452.2 mg (1.627 mmol) of <sup>n</sup>Bu<sub>4</sub>NCl was added and the solution was stirred for 10 min. The solution was purged for 15 min with N<sub>2</sub>. A 1-mL aliquot sample was retained as a dark control. Five-milliliter samples were transferred to a test tube and photolyzed with stirring under N<sub>2</sub> at 10 Hz with a Q-switch of 320 for 400 s. All the photolyzed samples were collected and stirred for 5 min and a 1-mL aliquot sample was retained as a photolyzed sample. The percent conversion was calculated through <sup>1</sup>H NMR integration between the dark control and the photolyzed sample against an internal standard of hexamethyldisiloxane. The rest of the photolyzed sample was neutralized with a saturated solution of NaHCO<sub>3</sub>, extracted with CH<sub>2</sub>Cl<sub>2</sub>, washed with H<sub>2</sub>O, dried with MgSO<sub>4</sub>, and filtered, and then the solvent was removed under reduced pressure. The sample was separated via flash column chromatography (240 mm  $\times$  36 mm) with 2% ether/hexanes. Fractions were tested by GC and collected and the solvent was removed under reduced pressure and weighed.

***N*-Methyl-1-aminonaphthalene (4).** 1-Aminonaphthalene (**3**, 5.23 g, 36.61 mmol) was dissolved in 25 mL of dry MeCN and then 5.01 g (35.33 mmol) of iodomethane was added to the solution while stirring. The solution was refluxed at 90 °C for 1 h with an ice water condenser. The mixture was then neutralized to pH 7 with a saturated solution of NaHCO<sub>3</sub> and extracted with CH<sub>2</sub>Cl<sub>2</sub> until the organic layer was colorless. The combined organic extracts were then dried over MgSO<sub>4</sub> and filtered, and the solvent was evaporated under reduced pressure to yield a dark purple oil. The monomethylated compound (**4**) was isolated through column chromatography (240 mm  $\times$  44 mm) and eluted with 15% EtOAc/85% hexanes. The correct fractions were collected and the solvent was evaporated under reduced pressure to yield 2.72 g (17.35 mmol, 47.39%) of a dark purple oil. <sup>1</sup>H NMR (400 MHz, CD<sub>3</sub>CN)  $\delta$  7.87 (d, *J* = 8 Hz, 1H), 7.76 (d, *J* = 8 Hz, 1H), 7.44–7.40 (m, 2H), 7.33 (t, *J* = 8 Hz, 1H), 7.15 (d, *J* = 8 Hz, 1H), 6.52 (d, *J* = 8 Hz, 1H), 5.08 (br s, 1H), 2.92 (d, *J* = 4 Hz, 3H); <sup>13</sup>C NMR (400 MHz, CDCl<sub>3</sub>)  $\delta$  144.4, 134.1, 128.5, 126.6, 125.6, 124.5, 123.3, 119.8, 117.0, 103.6, 30.8; UV–vis (MeCN) 215, 248, 333 nm; IR (CCl<sub>4</sub>) 3452 (m), 3068 (m), 3052 (m), 3013 (m), 2986 (m), 2940 (m), 2904 (m), 2881 (m), 2838 (m), 2815 (m), 1584 (s), 1522 (s) cm<sup>-1</sup>; MS (EI) *m/z* 157, 156, 128; HRMS (EI) calcd for C<sub>11</sub>H<sub>11</sub>N 157.0891, found 157.0886.

***N*-Methyl-*N*-nitroso-1-aminonaphthalene (5).** To the 2.72 g (17.35 mmol) of methylated compound **4** were added 6 g of ice and 3 mL of HCl on an ice bath. Immediately to this solution was added a solution of 1.51 g (21.90 mmol) of NaNO<sub>2</sub> in 10 mL distilled water that had been stirred for 10 min, and the resulting solution was stirred for 40 min to produce a maroon oil. The mixture was filtered and washed with H<sub>2</sub>O and CH<sub>2</sub>Cl<sub>2</sub>. The filtrate was neutralized to pH 7 with a saturated NaHCO<sub>3</sub> solution and extracted with CH<sub>2</sub>Cl<sub>2</sub> until the organic layer was colorless. The combined organic extracts were then dried over MgSO<sub>4</sub> and filtered, and the solvent was evaporated under reduced pressure. The nitrosated product (**5**) was isolated through column chromatography (240 mm  $\times$  44 mm) and eluted with 15% EtOAc/85% hexanes. The correct fractions were collected and the solvent was evaporated under reduced pressure to yield 2.64 g (14.19 mmol, 81.8%) of a dark tangerine oil. <sup>1</sup>H NMR (400 MHz, CD<sub>3</sub>CN)  $\delta$  8.06–7.96 (m, 2H), 7.70–7.28 (m, 5H), 3.51 (s, 3H); <sup>13</sup>C NMR (400 MHz, CDCl<sub>3</sub>)  $\delta$  138.9, 134.3, 129.8, 128.7, 128.4, 127.4, 126.7, 125.2,

(28) Novak, M.; Kennedy, S. A. *J. Am. Chem. Soc.* **1995**, *117*, 574–575.

(29) Kennedy, S. A.; Novak, M.; Kolb, B. A. *J. Am. Chem. Soc.* **1997**, *119*, 7654–7664.

(30) Purchase, I. F. H. K.; Ishmael, J.; Wilson, J.; Gore, C. W.; Chart, I. S. *Brit. J. Cancer* **1981**, *44*, 892–901.

(31) Radomski, J. L.; Deichmann, W. B.; Altman, N. H.; Radomski, T. *Cancer Res.* **1980**, *40*, 3537–3539.

(32) Frisch, M. J.; Trucks, G. W.; Schlegel, H. B.; Scuseria, G. E.; Robb, M. A.; Cheeseman, J. R.; Montgomery, J. A., Jr.; Vreven, T.; Kudin, K. N.; Burant, J. C.; Millam, J. M.; Iyengar, S. S.; Tomasi, J.; Barone, V.; Mennucci, B.; Cossi, M.; Scalmani, G.; Rega, N.; Petersson, G. A.; Nakatsuji, H.; Hada, M.; Ehara, M.; Toyota, K.; Fukuda, R.; Hasegawa, J.; Ishida, M.; Nakajima, T.; Honda, Y.; Kitao, O.; Nakai, H.; Klene, M.; Li, X.; Knox, J. E.; Hratchian, H. P.; Cross, J. B.; Adamo, C.; Jaramillo, J.; Gomperts, R.; Stratmann, R. E.; Yazyev, O.; Austin, A. J.; Cammi, R.; Pomelli, C.; Ochterski, J. W.; Ayala, P. Y.; Morokuma, K.; Voth, G. A.; Salvador, P.; Dannenberg, J. J.; Zakrzewski, V. G.; Dapprich, S.; Daniels, A. D.; Strain, M. C.; Farkas, O.; Malick, D. K.; Rabuck, A. D.; Raghavachari, K.; Foresman, J. B.; Ortiz, J. V.; Cui, Q.; Baboul, A. G.; Clifford, S.; Cioslowski, J.; Stefanov, B. B.; Liu, G.; Liashenko, A.; Piskorz, P.; Komaromi, I.; Martin, R. L.; Fox, D. J.; Keith, T.; Al-Laham, M. A.; Peng, C. Y.; Nanayakkara, A.; Challacombe, M.; Gill, P. M. W.; Johnson, B.; Chen, W.; Wong, M. W.; Gonzalez, C.; Pople, J. A. *Gaussian 03*; Gaussian, Inc.: Pittsburgh, PA, 2003.

(33) Becke, A. D. *Phys. Rev. A* **1988**, *38*, 3098–3100.

(34) Becke, A. D. *J. Chem. Phys.* **1993**, *98*, 5648–5652.

(35) Lee, C. T.; Yang, W. T.; Parr, R. G. *Phys. Rev. B* **1988**, *37*, 785–789.

(36) Stephens, P. J.; Devlin, F. J.; Chabalowski, C. F.; Frisch, M. J. *J. Phys. Chem.* **1994**, *98*, 11623–11627.

(37) Hehre, W. J.; Radom, L.; Schleyer, P. v. R.; Pople, J. A. *Ab Initio Molecular Orbital Theory*; Wiley: New York, 1986.

(38) Cioslowski, J. *J. Am. Chem. Soc.* **1989**, *111*, 8333–8336.

123.3, 122.0, 36.1; IR (CCl<sub>4</sub>) 3052 (s), 3017 (m), 2963 (m), 2931 (m), 2897 (m), 1953 (m), 1933 (m), 1809 (m) 1669 (m), 1596 (s), 1510 (s), 1448 (s), 1064 (s) cm<sup>-1</sup>; MS (EI) *m/z* 186, 156, 128; HRMS (EI) calcd for C<sub>11</sub>H<sub>10</sub>N<sub>2</sub>O 186.0793, found 186.0781.

**N-Methyl-N-(1-naphthyl)hydrazine (6).** AcOH, EtOH, and H<sub>2</sub>O (15 mL each) were stirred for 5 min, then the solution was added to 2.64 g (14.19 mmol) of the nitrosated compound (**5**) and the resulting solution again stirred for 5 min. To this solution, 3.71 g (56.75 mmol, 4 equiv) of Zn was added followed by stirring for 45 min. The solution was filtered to remove precipitated salts and rinsed with H<sub>2</sub>O and CH<sub>2</sub>Cl<sub>2</sub>. The filtrate was neutralized to pH 7 with both solid Na<sub>2</sub>CO<sub>3</sub> and aqueous NaHCO<sub>3</sub>. The solution was extracted with CH<sub>2</sub>Cl<sub>2</sub> until the organic layer was colorless. The combined organic extracts were dried over MgSO<sub>4</sub> and filtered, and the solvent was removed under reduced pressure yielding a dark purple oil. <sup>1</sup>H NMR (400 MHz, CD<sub>3</sub>CN) δ 8.30–8.28 (m, 1H), 7.83–7.80 (m, 1H), 7.54–7.38 (m, 4H), 7.26 (d, *J* = 7.6 Hz, 1H), 3.90 (br s, 2H), 3.02 (s, 3H); <sup>13</sup>C NMR (400 MHz, CDCl<sub>3</sub>) δ 150.6, 134.6, 128.2, 128.1, 125.8, 125.5, 125.4, 123.99, 123.96, 113.0, 49.1; IR (CCl<sub>4</sub>) 3351 (w) 3215 (w), 3048 (s), 2994 (m), 2947 (s), 2858 (w), 2838 (m), 2784 (s), 1914 (w), 1840 (w), 1813 (w), 1596 (s), 1572 (s), 1506 (s) cm<sup>-1</sup>; MS (EI) *m/z* 172, 157, 156, 128; HRMS (EI) calcd for C<sub>11</sub>H<sub>12</sub>N<sub>2</sub> 172.1000, found 172.0998.

**1-(N-Methyl-N-(1-naphthyl)amino)-2,4,6-trimethylpyridinium Tetrafluoroborate (1).** The percent yield of **5** was determined by the ratio of NMR integrations. To this crude product mixture was added 0.726 g (3.47 mmol) of freshly prepared **9**, followed by 10 mL of 100% EtOH. The solution was then stirred at room temperature for 2 h and cooled on an ice bath, then 200 mL of cold diethyl ether was added. Pale yellow crystals were isolated by filtration, giving 0.490 g (1.34 mmol, 38.61%) of **1**: mp 116–120 °C; <sup>1</sup>H NMR (400 MHz, CD<sub>3</sub>CN) δ 7.96 (d, *J* = 4.2 Hz, 1H), 7.74 (d, *J* = 4.2 Hz, 1H), 7.65 (s, 2H), 7.55–7.37 (br m, 3H), 3.72 (s, 3H), 2.64 (s, 6H), 2.55 (s, 3H); <sup>13</sup>C NMR (400 MHz, CDCl<sub>3</sub>) δ 159.8, 157.3, 140.4, 135.3, 130.1, 129.6, 126.9, 126.6, 125.86, 125.6, 125.2, 124.6, 113.6, 21.9, 20.5, 19.6; UV–vis (MeCN) 267, 281, 299, 347 nm; ε<sub>266</sub> 7287 M<sup>-1</sup> cm<sup>-1</sup>, ε<sub>355</sub> 2044 M<sup>-1</sup> cm<sup>-1</sup>; IR (Nujol) 2959 (m), 2947 (m), 2924 (s), 2908 (m), 2889 (w), 2854 (m), 2842 (w), 1456 (m) 1374 (m) cm<sup>-1</sup>; MS (FAB) *m/z* (rel intensity) 277.2 (14), 156.1 (100), 127 (3); HRMS (FAB) calcd for C<sub>19</sub>H<sub>21</sub>N<sub>2</sub> [M – BF<sub>4</sub>]<sup>+</sup> 277.170465, found 277.17047.

**4-Chloro-N-methyl-N-1-aminonaphthalene (7).** 1-Amino-4-chloronaphthalene (0.82 g, 4.62 mmol) was dissolved in 25 mL of dry MeCN and then 0.638 g (4.49 mmol, 0.974 equiv) of iodomethane was added to the solution with stirring. The solution was refluxed at 90 °C for 30 min with an ice water condenser. The mixture was then neutralized to pH 7 with a saturated solution of NaHCO<sub>3</sub> and extracted with CH<sub>2</sub>Cl<sub>2</sub> until the organic layer was colorless. The combined organic extracts were then dried over MgSO<sub>4</sub> and filtered, and the solvent was evaporated under reduced pressure to yield a dark orange oil. The monomethylated compound (**3**) was isolated through column chromatography (240 mm × 44 mm) and eluted with 15% EtOAc/85% hexanes. The correct fractions were collected and the solvent was evaporated under reduced pressure to yield 0.139 g (0.728 mmol, 15.79%) of a dark purple oil. <sup>1</sup>H NMR (400 MHz, CD<sub>3</sub>CN) δ: 8.14 (d, *J* = 8.4 Hz, 1H), 7.94 (d, *J* = 8.4 Hz, 1H), 7.60 (t, *J* = 8 Hz, 1H), 7.51 (t, *J* = 8.2 Hz, 1H), 7.43 (d, *J* = 8.4 Hz, 1H), 6.47 (d, *J* = 8 Hz, 1H), 5.24 (br s, 1H), 2.91 (d, *J* = 5.2, 3H); <sup>13</sup>C NMR (400 MHz, CDCl<sub>3</sub>) δ 143.8, 131, 126.7, 125.3, 125.2, 124.4, 120.1, 119.9, 103.7, 31; IR (CCl<sub>4</sub>) 3452 (m), 3075 (m), 3044 (m), 2982 (m), 2935 (s), 2904 (m), 2885 (w) 2819 (m), 1817 (w), 1572 (s), 1378 (s), 1079 (m), 1033 (m) cm<sup>-1</sup>; MS (FAB) *m/z* 191, 176, 156; HRMS (FAB) calcd for C<sub>11</sub>H<sub>10</sub>NCl 191.050173, found 191.05017.

**2-Chloro-N-methyl-N-1-aminonaphthalene (8).** Yellow oil was isolated. <sup>1</sup>H NMR (400 MHz, CD<sub>3</sub>CN) δ 8.15 (d, *J* = 8.4 Hz, 1H), 7.84 (d, *J* = 3.8 Hz, 1H), 7.54–7.39 (m, 4H), 4.29 (br s, 1H), 2.98 (s, 3H); <sup>13</sup>C NMR (400 MHz, CDCl<sub>3</sub>) δ 143.1, 133.5, 128.4, 126.8, 125.9, 123.8, 123.1, 121.9, 30.3; IR (CCl<sub>4</sub>) 3646 (w), 3060 (w), 2959 (s), 2920 (s), 2858 (s), 1728 (w), 1553 (s), 1549 (s), 1258 (s), 1099 (s), 1013(s) cm<sup>-1</sup>; MS (EI) *m/z* (rel intensity) 191 (100), 176 (13), 156 (16); HRMS (EI) calcd for C<sub>11</sub>H<sub>10</sub>NCl 191.050173, found 191.0504

**Acknowledgment.** This work was supported by the Chemistry Division of the National Science Foundation.

**Supporting Information Available:** <sup>1</sup>H and <sup>13</sup>C NMR spectra for compounds **1** and **4–8**, COSY-<sup>1</sup>H NMR for compound **8**, and Cartesian coordinates for DFT calculations for compounds **2** and **10–12**. This material is available free of charge via the Internet at <http://pubs.acs.org>.

JO0477749